nature climate change

SUPPLEMENTARY INFORMATION

DOI: 10.1038/NCLIMATE3241

In the format provided by the authors and unedited.

Influence of high-latitude atmospheric circulation changes on summertime Arctic sea ice

Qinghua Ding[1,2,3]*, Axel Schweiger[3], Michelle L'Heureux[4], David S. Battisti[5,6], Stephen Po-Chedley[5], Nathaniel C. Johnson[7], Eduardo Blanchard-Wrigglesworth[5], Kirstin Harnos[4], Qin Zhang[4], Ryan Eastman[5] and Eric J. Steig[5,6]

[1]Department of Geography, University of California, Santa Barbara, California 93106, USA. [2]Earth Research Institute, University of California, Santa Barbara, California 93106, USA. [3]Polar Science Center, Applied Physics Laboratory, University of Washington, Seattle, Washington 98195, USA. [4]NOAA Climate Prediction Center, College Park, Maryland 20740, USA. [5]Department of Atmospheric Sciences, University of Washington, Seattle, Washington 98195, USA. [6]Department of Earth and Space Sciences, University of Washington, Seattle, Washington 98195, USA. [7]Cooperative Institute for Climate Science, Princeton University, Princeton, New Jersey 08540, USA. *e-mail: qinghua@ucsb.edu

Supplementary Figures for Ding et al., "Influence of high-latitude atmospheric …"

This document includes the Supplementary Figures that are referred to in the main text.

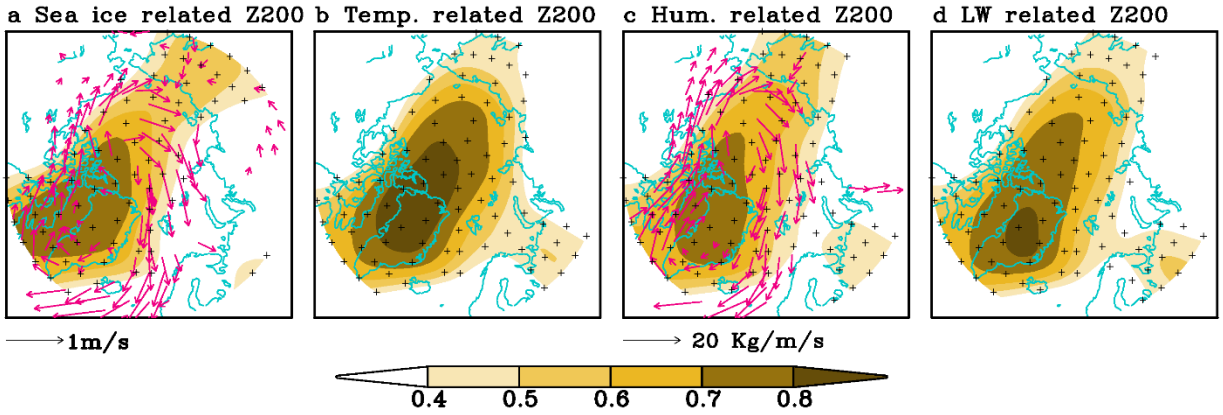

Supplementary Fig. 1 Same as Fig. 1 d) to g), but using raw data in calculating the correlation. Stippling indicates statistical significant correlation at the 5% level.

Supplementary Figures for Ding et al., "Influence of high-latitude atmospheric …"

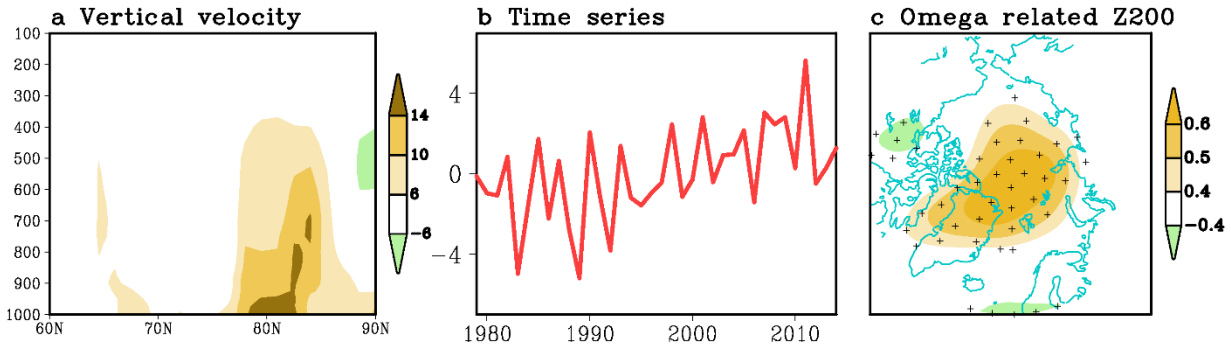

Supplementary Fig 2 a) Meridional cross section of linear trend of zonal mean JJA vertical velocity (10^{-5} Pa/s/decade) in ERA-I (1979-2014). b) Domain averaged JJA lower level vertical velocity (1000hPa to 700hPa, unit: 10^{-5} Pa/s) in the Arctic (north of 70ºN). c) Correlation of omega index in (b) with JJA Z200 in 1979-2014. The trends are removed before the calculation. In c) stippling indicates statistical significant correlation at the 5% level.

Supplementary Figures for Ding et al., "Influence of high-latitude atmospheric …"

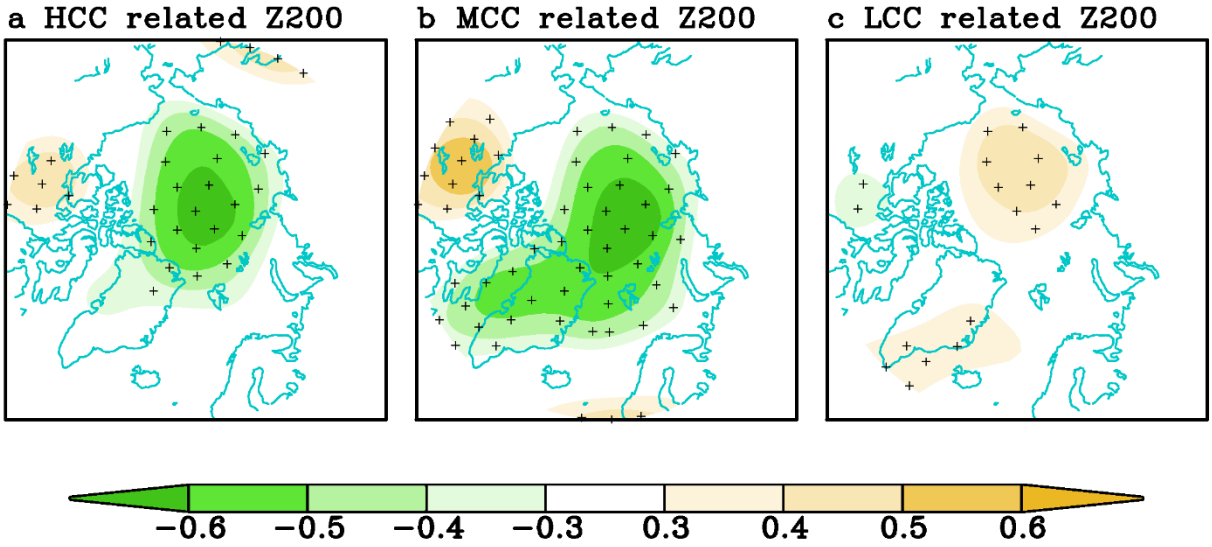

Supplementary Fig 3. Correlation of a domain (north of 70ºN) averaged JJA cloudiness index in the upper level (HCC), middle level (MCC) and lower level (LCC) with JJA Z200 (a to c) in 1979-2014. The trends are removed before the calculation**.** Cloud data is from the ERA-I reanalysis. Stippling indicates statistical significant correlation at the 5% level.

Supplementary Figures for Ding et al., "Influence of high-latitude atmospheric …"

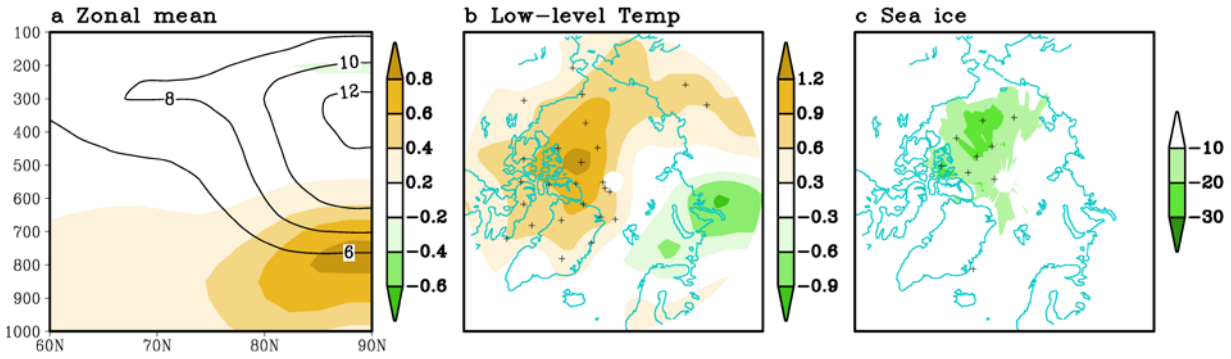

Supplementary Fig 4: Linear trends of a) meridional cross section of zonal mean JJA temperature (shading, ºC per decade) and geopotential height (black contour, m per decade, b) JJA lower level temperature (100hPa-750hPa) and c) September sea ice (% per decade) simulated in Exp-3 in which the model is nudged to observed ERA-I winds above 700hPa. Stippling indicates statistical significant trends at the 5% level.

Supplementary Figures for Ding et al., "Influence of high-latitude atmospheric …"

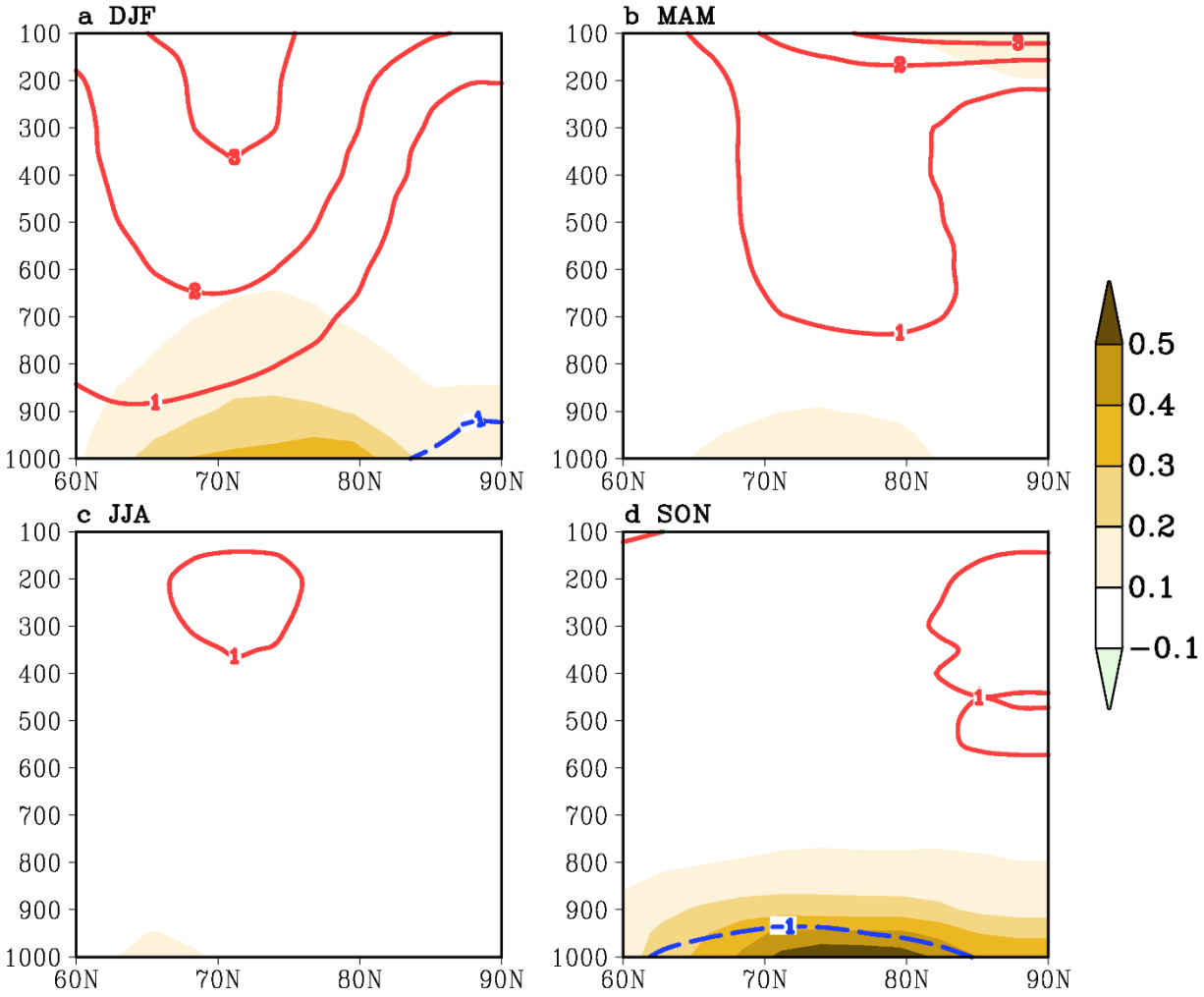

Supplementary Fig. 5 Meridional cross section of linear trend of zonal mean temperature (shading: ºC per decade) and geopotential height (contour: m per decade) in Exp-4 (1979-2014) in each season.

Supplementary Figures for Ding et al., "Influence of high-latitude atmospheric …"

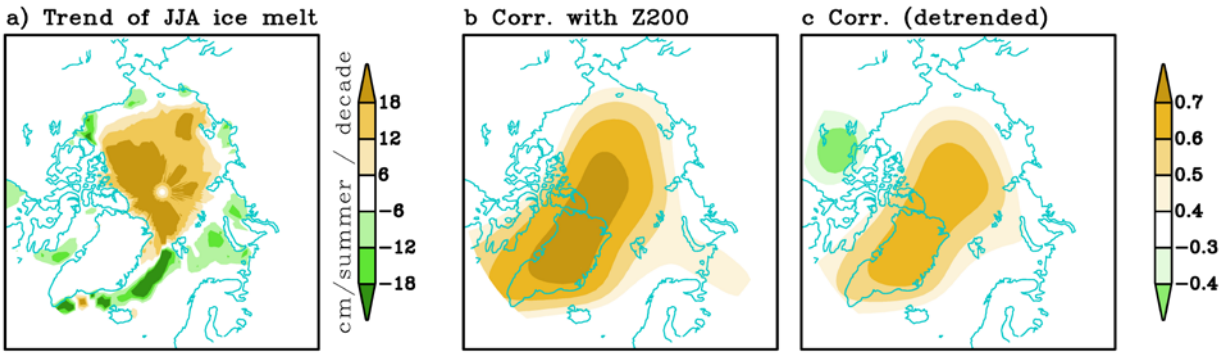

Supplementary Fig. 6: a) Linear trend of JJA total sea ice melting in POP2-CICE4 run forced by ERA-I forcing during 1979-2014 period (Exp-5).b) Correlation between the domain averaged JJA total melting in the Arctic (north of 70ºN) and JJA Z200 during the period 1979-2014. c) same as b) but using the detrended components of the melting index and JJA Z200 in the Arctic.

Supplementary Figures for Ding et al., "Influence of high-latitude atmospheric …"

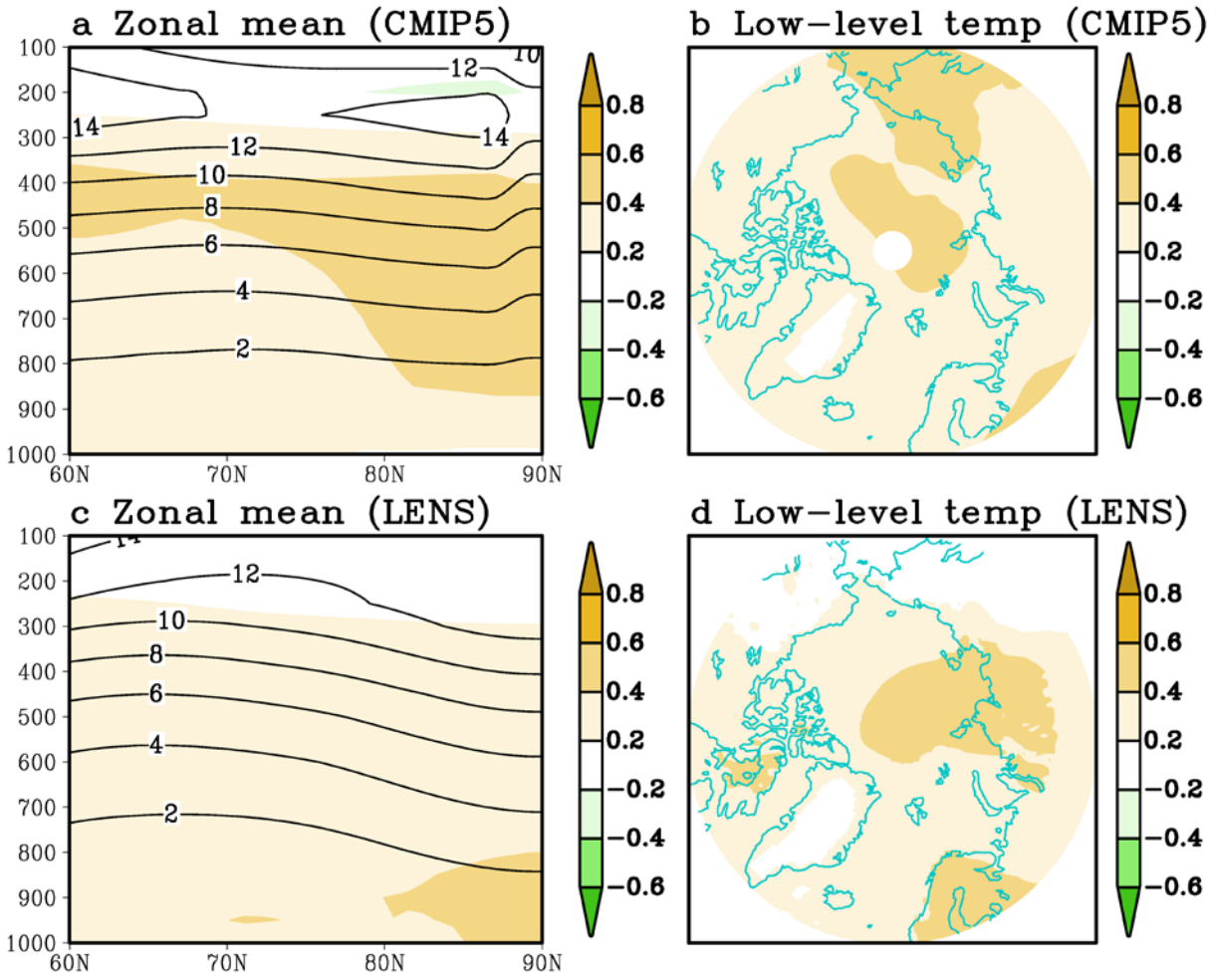

Supplementary Fig. 7 a) & c) Meridional cross section of the linear trend of zonal mean JJA temperature (shading: ºC per decade) and geopotential height (contour: m per decade) in CMIP5 projects (1979-2014, upper panels) and CESM LENS (1979-2014, lower panels); b) &d) Linear trend of lower tropospheric (surface to 750hPa) JJA temperature (ºC per decade) in CMIP5 (1979-2014) and CESM LENS (1979-2014).

Supplementary Figures for Ding et al., "Influence of high-latitude atmospheric …"

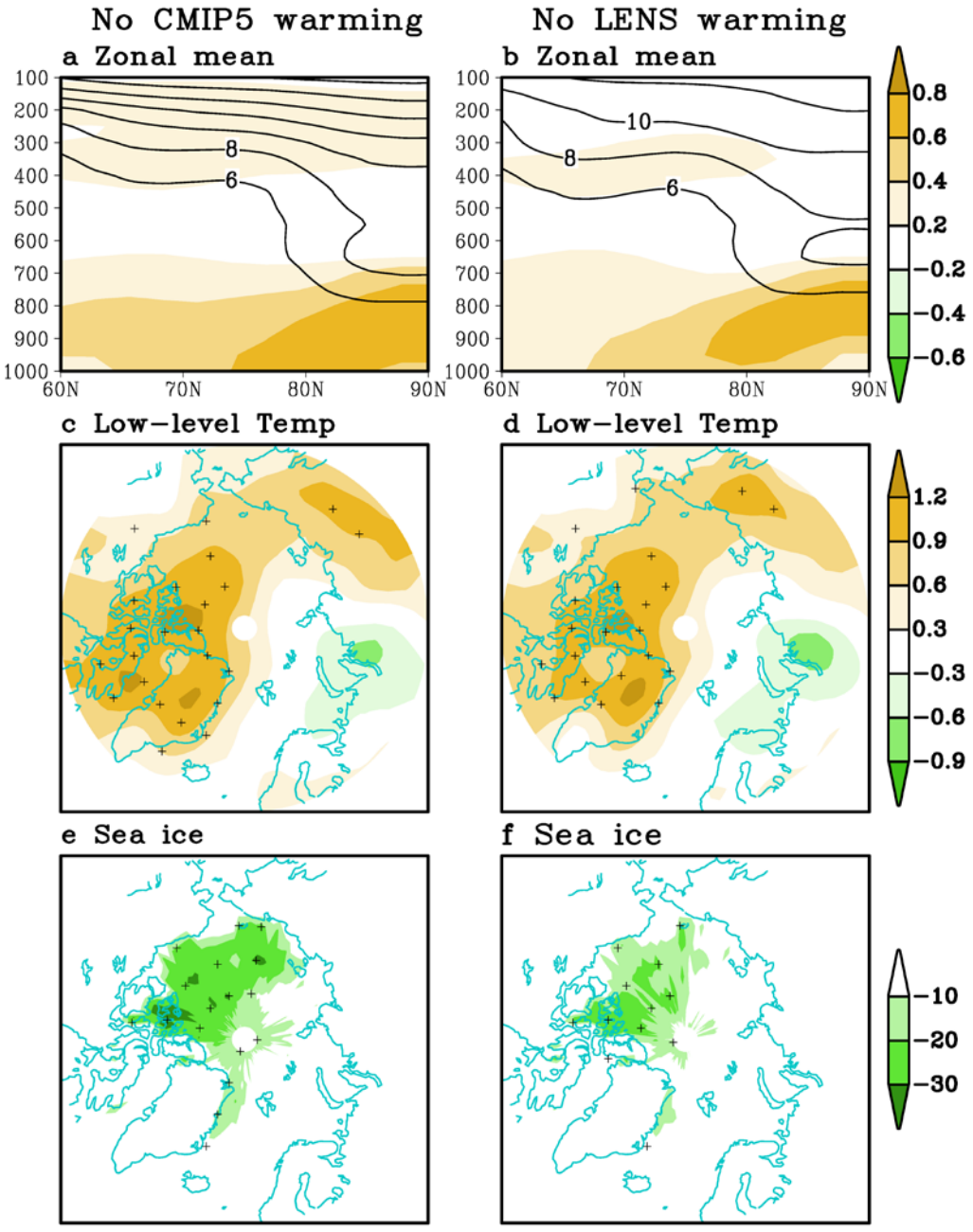

Supplementary Fig. 8: Linear trends of a) & b) meridional cross section of zonal mean JJA temperature (shading, ºC per decade) and geopotential height (black contour, m per decade, c) & d) JJA lower level temperature (1000hPa-750hPa) and e) & f) September sea ice (% per decade) simulated in two ECHAM5 nudged experiments (Exp-7 and 8) in which the global wind patterns (zonal and meridional) forced by anthropogenic forcing in CMIP5 (left column) and LENS (right column) projects are removed from ERA-I observed winds.

Supplementary Figures for Ding et al., "Influence of high-latitude atmospheric …"

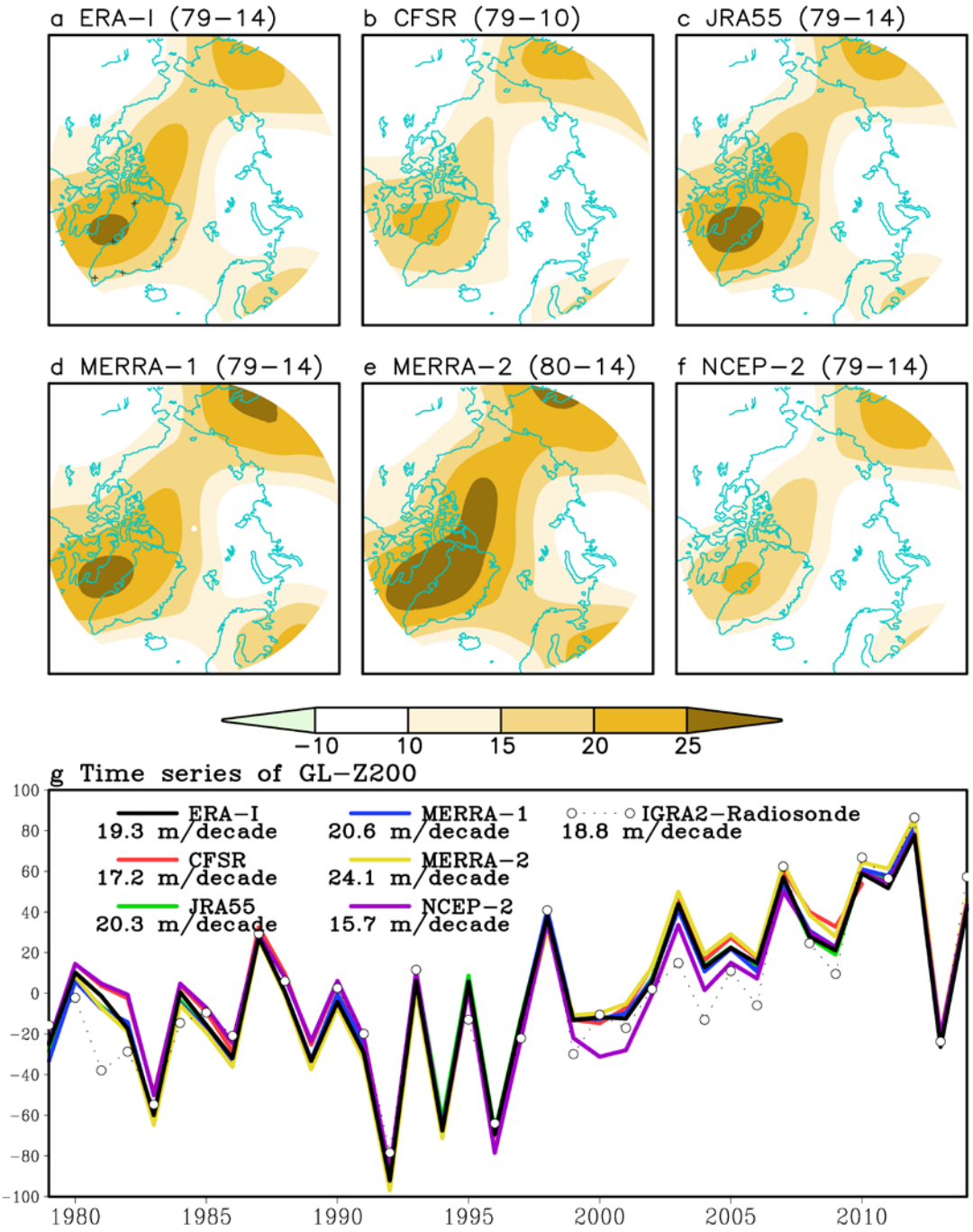

Supplementary Fig. 9: a) to f) Linear trends of JJA Z200 from six different reanalysis datasets and the time series of g) GL-Z200 derived from each reanalysis and six IGRA2 radiosonde stations (location of the stations is marked in panel a, 1989&1994 data are not used because data in this two years doesn't pass the quality control). Linear trend of each index (m/decade) is denoted below its name.

Supplementary Figures for Ding et al., "Influence of high-latitude atmospheric …"

Supplementary Table 1: 26 climate models in the CMIP5 historical experiment. List of 26 CMIP5 CGCMs used in Fig. 4 to examine the forced response of the climate system to anthropogenic and natural external forcing, along with the number of atmospheric horizontal grids.

CMIP5 model designation	nx	ny
1. ACCESS1-0	192	144
2. ACCESS1-3	192	144
3. bcc-csm1-1	128	64
4. bcc-csm1-1-m	320	160
5. BNU-ESM	128	64
6. CCSM4	288	192
7. CNRM-CM5	256	128
8. CSIRO-Mk3-6-0	192	96
9. CanESM2	128	64
10. FGOALS-g2	128	60
11. GFDL-CM3	144	90
12. GFDL-ESM2G	144	90
13. GFDL-ESM2M	144	90
14. GISS-E2-H	144	89
15. GISS-E2-R	144	89
16. HadGEM2-AO	192	144
17. inmcm4	180	120
18. IPSL-CM5A-LR	96	96
19. IPSL-CM5A-MR	144	143
20. IPSL-CM5B-LR	96	96
21. MIROC-ESM	128	64
22. MIROC5	256	128
23. MPI-ESM-LR	192	96
24. MPI-ESM-MR	192	96
25. MRI-CGCM3	320	160
26. NorESM1-ME	144	96